

Spin-orbit alignment of exoplanet systems: how can Asteroseismology help us?

Tiago L. Campante^{1,2}

¹School of Physics and Astronomy, University of Birmingham,
Edgbaston, Birmingham, B15 2TT, UK
email: campante@bison.ph.bham.ac.uk

²Stellar Astrophysics Centre (SAC), Department of Physics and Astronomy,
Aarhus University, Ny Munkegade 120, DK-8000 Aarhus C, Denmark

Abstract. Measuring the obliquities of exoplanet-host stars provides invaluable diagnostic information for theories of planetary formation and migration. Most of these results have so far been obtained by measuring the Rossiter–McLaughlin effect, clearly favoring systems that harbor hot Jupiters. While it would be extremely helpful to extend these measurements to long-period and multiple-planet systems, it is also true that the latter systems tend to involve smaller planets, making it ever so difficult to apply such techniques. Asteroseismology provides a powerful method of determining the inclination of the stellar spin axis from an analysis of the rotationally-induced splittings of the oscillation modes. This provides an estimate of the obliquity independently of other methods. The applicability of the asteroseismic method is determined by the stellar properties and not by the signal-to-noise ratio of the transit data. Here we present a recap of the spin-orbit geometry, explain how the asteroseismic method works, and review previous applications of the method to exoplanet-host stars.

Keywords. asteroseismology, methods: statistical, planetary systems, planets and satellites: general, stars: solar-type, techniques: photometric

1. Introduction

The spin-orbit angle ψ has been recognized as an important diagnostic of theories of planet formation, migration, and tidal evolution. For practical reasons, most obliquity measurements to date have been for systems harboring hot Jupiters (e.g., Albrecht *et al.* 2012). In order to study the dynamical histories of planetary systems across a wider range of architectures, it is, however, imperative to extend these measurements to systems with smaller planets, longer-period planets, and multiple planets. An alternative technique for measuring the obliquities of planetary systems, one that does not depend on the signal-to-noise ratio (S/N) of the transit data, is asteroseismology. The asteroseismic estimation of the stellar inclination angle rests on our ability to resolve and extract signatures of rotation in the power spectra of non-radial modes of oscillation. Its applicability depends entirely on the stellar properties, namely, on the intrinsic ratio ν_s/Γ between the rotational splitting and the full width at half maximum (or linewidth) of the oscillation mode profiles, and not on the planetary or orbital parameters, which is a clear advantage when measuring the obliquities of systems with small planets or long-period planets.

2. Spin-orbit geometry

In Fig. 1, z points toward the observer and the xy plane is the plane of the sky. Moreover, \mathbf{n}_o and \mathbf{n}_s denote the orbital and stellar angular momentum vectors, respectively.

For a transiting planet, the orbital inclination i_o is measurable via transit photometry, while the projected spin-orbit angle λ is measurable via the Rossiter–McLaughlin effect or the analysis of planetary transits over starspots. In addition, the stellar inclination i_s can in principle be constrained using asteroseismology. Nevertheless, we should keep in mind that the only angle of intrinsic physical significance is the true obliquity or spin-orbit angle, ψ , between \mathbf{n}_o and \mathbf{n}_s , which is generally not directly measurable.

The various angles are related according to (Fabrycky & Winn 2009):

$$\cos \psi = \sin i_s \cos \lambda \sin i_o + \cos i_s \cos i_o. \quad (2.1)$$

For a transiting system, we would still expect to place mild constraints on ψ even when lacking a measurement of λ . In Fig. 2 we show the posterior probability distribution for ψ conditioned on i_s and i_o , $p(\psi|i_s, i_o)$, sampled by means of Monte Carlo simulations using Eq. (2.1). We have assumed an edge-on orbit ($i_o = 90^\circ$), having selected three error-free values for the stellar inclination ($i_s = 30^\circ$, $i_s = 60^\circ$, and $i_s = 85^\circ$). A uniform distribution in λ was used to express our ignorance with respect to this quantity. We have also derived a potentially useful analytical expression for $p(\psi|i_s, i_o)$ (T. L. Campante *et al.*, submitted),

$$p(\psi|i_s, i_o) \propto \frac{\sin i_s \sin \psi}{\sqrt{\sin^2 \psi \sin^2 i_o - (\cos \psi \cos i_o - \cos i_s)^2}}, \quad \text{for all } |i_o - i_s| < \psi < i_o + i_s, \quad (2.2)$$

that we plot in Fig. 2. The main conclusions to be drawn from this simple exercise follow immediately from an inspection of Fig. 2: For a transiting system, a small value of i_s implies a spin-orbit misalignment. The converse is not true, since a large value of i_s is consistent with, but does not necessarily imply, a spin-orbit alignment. For instance, if we consider $i_s = 85^\circ$, then any spin-orbit angle in the range $5^\circ < \psi < 175^\circ$ has a nonnegligible probability. The interpretation of the spin-orbit alignment in terms of the measured i_s can thus be ambiguous. Therefore, in order to draw general inferences about spin-orbit alignment, a statistical analysis of an ensemble of such measurements is needed (Fabrycky & Winn 2009; Morton & Winn 2014).

3. Estimation of the stellar inclination angle via asteroseismology

Solar-like oscillations are predominantly acoustic global standing waves. Commonly called p modes, owing to the fact that pressure plays the role of the restoring force, these modes are intrinsically damped and stochastically excited by near-surface convection. Consequently, all stars cool enough to have an outer convective envelope may be expected to exhibit solar-like oscillations. The oscillation modes are characterized by the radial order n (related to the number of radial nodes), the spherical degree l (specifying the number of nodal surface lines), and the azimuthal order m (with $|m|$ specifying how many of the nodal surface lines cross the equator). Radial modes have $l=0$, whereas non-radial modes have $l>0$. Values of m range from $-l$ to l , meaning that there are $2l+1$ azimuthal components for a given multiplet of degree l . Observed oscillation modes are typically high-order modes of low spherical degree.

The asteroseismic estimation of i_s rests on our ability to resolve and extract signatures of rotation in the power spectra of non-radial modes of oscillation. Rotation lifts the degeneracy in the frequencies, ν_{nl} , of non-radial modes and introduces a dependence of the oscillation frequencies on m , with prograde (retrograde) modes (with $m > 0$ and $m < 0$, respectively) having frequencies slightly higher (lower) than the axisymmetric mode ($m = 0$) in the observer's frame of reference. For the fairly modest values of the stellar angular velocity Ω that are typical of solar-like oscillators, the effect of rotation can

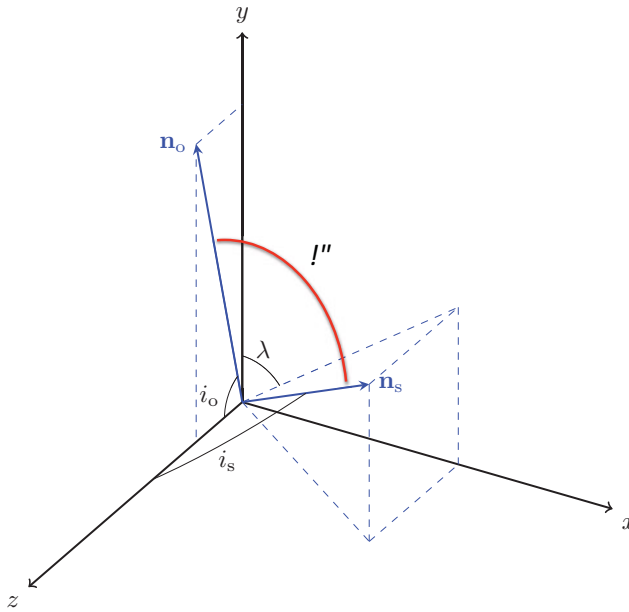


Figure 1. Observer-oriented coordinate system. Here the z axis points toward the observer, the x axis points along the line of nodes, the y axis completes a right-handed triad, and the xy plane is the plane of the sky. The unit vectors \mathbf{n}_o and \mathbf{n}_s denote the orbital and stellar angular momentum unit vectors, respectively. All depicted angles are introduced in the text.

be treated following a perturbative analysis and the star is generally assumed to rotate as a solid body (i.e., $\Omega = \text{const.}$). In the limit of solid-body rotation, the frequency ν_{nlm} of a mode, as observed in an inertial frame, can be expressed to first order as (Ledoux 1951):

$$\nu_{nlm} = \nu_{nl0} + m \frac{\Omega}{2\pi} (1 - C_{nl}) \approx \nu_{nl0} + m\nu_s. \quad (3.1)$$

The kinematic splitting $m\Omega/(2\pi)$ is corrected for the effect of the Coriolis force through the dimensionless Ledoux constant, C_{nl} . For high-order p modes, $C_{nl} \ll 1$, with the rotational splitting being dominated by advection and given approximately by the angular velocity, i.e., $\nu_s \approx \Omega/(2\pi)$. To a second order of approximation, centrifugal effects that disrupt the equilibrium structure of the star can be taken into account through an additional frequency perturbation (e.g., Ballot 2010). This perturbation scales as the ratio of the centrifugal to the gravitational forces at the stellar surface, i.e., $\Omega_{\text{surf}}^2 R_s^3 / (GM_s)$, where G is the gravitational constant, R_s is the stellar radius, and M_s is the stellar mass.

Assuming energy equipartition between multiplet components with different azimuthal order, the dependence of mode power on m is given by (e.g., Gizon & Solanki 2003):

$$\mathcal{E}_{lm}(i_s) = \frac{(l - |m|)!}{(l + |m|)!} \left[P_l^{|m|}(\cos i_s) \right]^2, \quad (3.2)$$

where $P_l^m(x)$ are the associated Legendre functions and the sum over m of $\mathcal{E}_{lm}(i_s)$ has been normalized to unity. Measurement of the relative power of the azimuthal components in a non-radial multiplet thus provides a direct estimate of the stellar inclination angle. The above formalism further relies on the assumption that contributions to the observed intensity across the visible stellar disk depend only on the angular distance from the disk center, which is valid for photometric observations. According to Eq. (3.2), when the

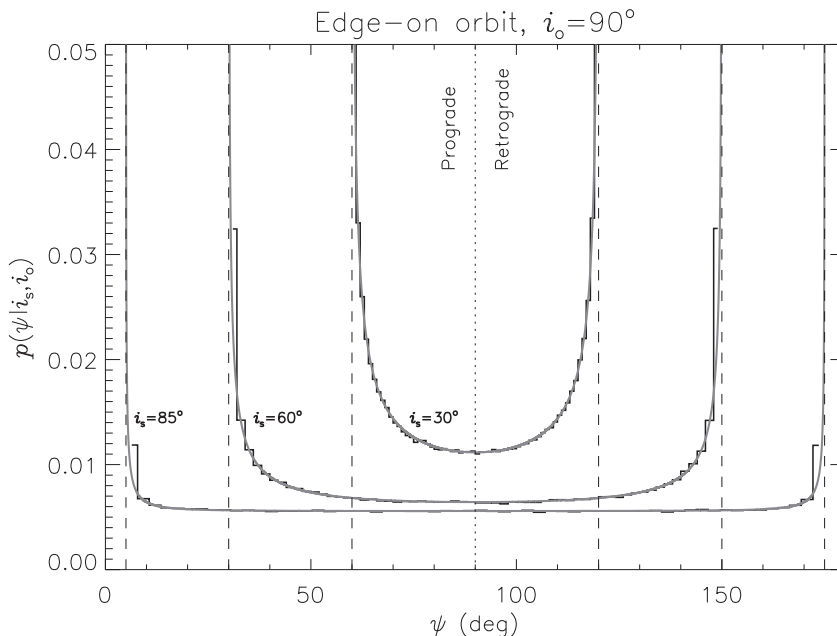


Figure 2. Posterior probability distribution for the spin-orbit angle ψ conditioned on i_s and i_o , $p(\psi|i_s, i_o)$. The posterior distributions have been sampled by means of Monte Carlo simulations using Eq. (2.1) and are displayed as histograms. The analytical expression for $p(\psi|i_s, i_o)$ given in Eq. (2.2) is plotted (after normalization) in gray. The vertical dashed lines are placed at the asymptotes $\psi = |i_o - i_s|$ and $\psi = i_o + i_s$. The vertical dotted line at $\psi = \pi/2$ marks the transition between a prograde and a retrograde orbit.

stellar spin axis points toward the observer (pole-on configuration), only the axisymmetric mode is visible and no inference can thus be made about rotation. When the spin axis lies on the plane of the sky (edge-on configuration), as is approximately the case of the Sun, observations are essentially sensitive only to modes with even $|l - m|$. Figure 3 displays the theoretical profiles of dipole ($l = 1$) modes as a function of the angle i_s for three different ν_s/Γ ratios. Dipole modes are approximately three times more prominent in the power spectra of intensity observations than quadrupole ($l = 2$) modes of similar frequency, and consequently it is the former modes that ultimately determine our ability to constrain i_s . It is evident from Fig. 3 that, given sufficient frequency resolution and S/N, it will be the intrinsic ratio ν_s/Γ which determines whether it is possible to resolve the azimuthal components (Ballot, García & Lambert 2006).

A detailed fitting of the modes of oscillation to extract signatures of rotation from the power spectrum is normally done in a Bayesian manner using an MCMC (Markov chain Monte Carlo; e.g., Handberg & Campante 2011) or similar sampler. Analytical approximations for the errors on i_s and ν_s are given in Ballot *et al.* (2008). Bayesian inference, however, is capable of providing us with the full posterior probability distribution (ppd) of these parameters, from which credible regions can be conveniently defined. We note that even though i_s is independent of ν_s , their measured values are highly correlated. The ppd of i_s can then be used to sample that of the spin-orbit angle ψ via Eq. (2.1).

Broad mode profiles (characteristic of late F-type stars) hinder our ability to resolve and extract signatures of rotation in the power spectrum. When coupled to a moderate-to-low S/N in the p modes, this means that the effect of the correlated background noise on the mode profiles may bias the outcome of the detailed fitting analysis. A

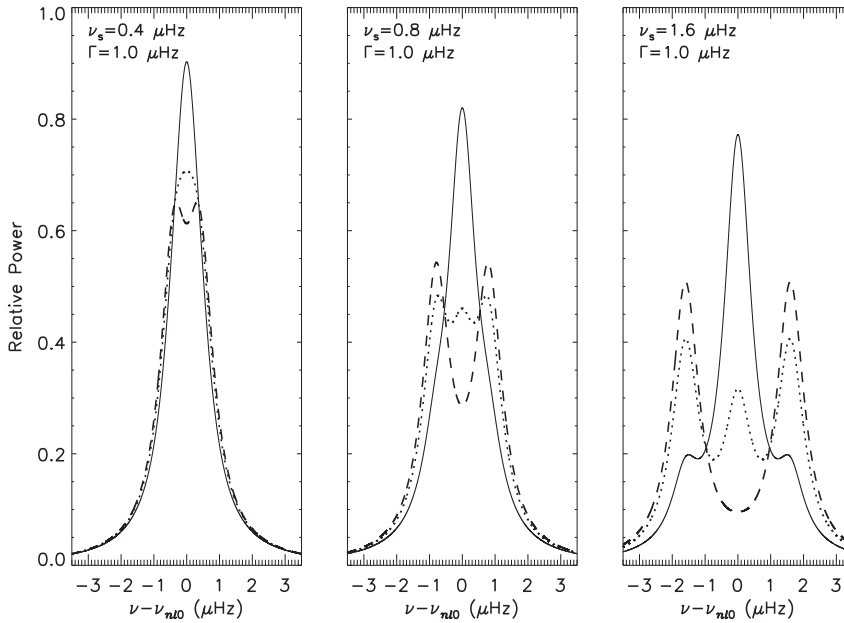


Figure 3. Theoretical profiles of dipole multiplets as a function of i_s for three different ν_s/Γ ratios. The linewidths of the mode profiles of the azimuthal components have been assigned solar values ($\Gamma = 1.0 \mu\text{Hz}$). The rotational splitting ranges from solar ($\nu_s = 0.4 \mu\text{Hz}$; left-hand panel) to twice (middle panel) and four times (right-hand panel) solar. The three stellar inclination angles are represented by different line styles: $i_s = 30^\circ$ (solid), $i_s = 60^\circ$ (dotted), and $i_s = 85^\circ$ (dashed).

reduced visibility of the multiplet components is an issue that is frequently encountered. In order to test the asteroseismic method, and in particular the robustness of the returned uncertainties on i_s , we recommend that in such situations tests with artificial data be performed.

4. Applications

Following the application of the asteroseismic technique to a few host stars with single, non-transiting large planets discovered using the radial-velocity method (Wright *et al.* 2011; Gizon *et al.* 2013), the asteroseismic technique has recently been applied to several Sun-like hosts observed with NASA's *Kepler* space telescope (Chaplin *et al.* 2013; Benomar *et al.* 2014; Lund *et al.* 2014; Van Eylen *et al.* 2014). In addition, Huber *et al.* (2013) used asteroseismology to measure a large obliquity for Kepler-56, a red giant hosting two transiting coplanar planets, thus showing that spin-orbit misalignments are not confined to hot-Jupiter systems. Another instance of an asteroseismic obliquity measurement of an evolved host star is that of Kepler-432 (Quinn *et al.* 2015), for which the obliquity of one of its two long-period giant planets may have been shaped by the same process that realigns hot-Jupiter systems. Recently, the stellar inclination angles of the solar analogs 16 Cyg A and B were determined using asteroseismology by Davies *et al.* (2015). The B component hosts a Jovian planet in an eccentric, low-obliquity orbit, which is consistent with Kozai cycling driven by the A component. The first statistical analysis of an ensemble of asteroseismic obliquity measurements obtained for solar-type stars hosting transiting planets was recently conducted (T. L. Campante *et al.*, submitted).

References

- Albrecht, S., Winn, J. N., Johnson, J. A., *et al.* 2012, *ApJ*, 757, 18
- Ballot, J., García, R. A., & Lambert, P. 2006, *MNRAS*, 369, 1281
- Ballot, J., Appourchaux, T., Toutain, T., & Guittet, M. 2008, *A&A*, 486, 867
- Ballot, J. 2010, *Astronomische Nachrichten*, 331, 933
- Benomar, O., Masuda, K., Shibahashi, H., & Suto, Y. 2014, *PASJ*, 66, 94
- Chaplin, W. J., Sanchis-Ojeda, R., Campante, T. L., *et al.* 2013, *ApJ*, 766, 101
- Davies, G. R., Chaplin, W. J., Farr, W. M., *et al.* 2015, *MNRAS*, 446, 2959
- Fabrycky, D. C. & Winn, J. N. 2009, *ApJ*, 696, 1230
- Gizon, L. & Solanki, S. K. 2003, *ApJ*, 589, 1009
- Gizon, L., Ballot, J., Michel, E., *et al.* 2013, *Proc. of the National Academy of Science*, 110, 13267
- Handberg, R. & Campante, T. L. 2011, *A&A*, 527, A56
- Huber, D., Carter, J. A., Barbieri, M., *et al.* 2013, *Science*, 342, 331
- Ledoux, P. 1951, *ApJ*, 114, 373
- Lund, M. N., Lundkvist, M., Silva Aguirre, V., *et al.* 2014, *A&A*, 570, A54
- Morton, T. D. & Winn, J. N. 2014, *ApJ*, 796, 47
- Quinn, S. N., White, T. R., Latham, D. W., *et al.* 2015, *ApJ*, 803, 49
- Van Eylen, V., Lund, M. N., Silva Aguirre, V., *et al.* 2014, *ApJ*, 782, 14
- Wright, D. J., Chené, A.-N., De Cat, P., *et al.* 2011, *ApJ* (Letters), 728, L20